J Pharmacokinet Pharmacodyn (2010) 37:591–615
DOI 10.1007/s10928-010-9185-x

Physiologically-based pharmacokinetic modeling for absorption, transport, metabolism and excretion

K. Sandy Pang · Matthew R. Durk

Received: 6 September 2010 / Accepted: 12 November 2010 / Published online: 14 December 2010

Abstract The seminal paper on the liver physiologically-based pharmacokinetic (PBPK) model by Rowland et al. (J Pharmacokinet Biopharm 1:123–136, 1973) that described the influence of blood flow, intrinsic clearance, and binding on hepatic clearance had inspired further development of PBPK modeling of the liver, kidney and intestine as well as whole body. Shortly thereafter, a series of papers from Pang and Rowland compared the well-stirred and parallel-tube liver models and sparked further development on clearance concepts in the liver, including those described by the dispersion model. From 2005 onwards, several seminal papers by Rodgers and Rowland, in their recognition of the binding of molecules to tissue acidic and neutral phospholipids, improved the methodology in providing estimates of the tissue-to-plasma coefficient and rendering easy calculation of these hard-to-get constants. The improvement has strongly consolidated the basic premise on PBPK modeling and simulations and these basics have allowed scientists to focus on other important variables: membrane barriers, and transporter and enzyme and their heterogeneities that further impact drug disposition. In particular, the PBPK models have delved into sequential metabolism and futile cycling to illustrate how transporters and enzymes could affect the metabolism of drugs and metabolites. PBPK models that are especially pertinent to metabolite kinetics are being utilized in drug studies and risk assessment. These types of PBPK modeling reveal differences in

K. S. Pang (✉) · M. R. Durk
Leslie Dan Faculty of Pharmacy, University of Toronto,
144 College Street, Toronto, ON M5S 3M2, Canada
e-mail: ks.pang@utoronto.ca

M. R. Durk
e-mail: matthew.durk@utoronto.ca

kinetics between the formed vs. preformed metabolite, showing special considerations for membrane barriers, and the influence of competing pathways and competing organs.

Keywords Physiologically-based pharmacokinetic (PBPK) modeling · Metabolite kinetics · Sequential metabolism · Absorption, transport and excretion

Introduction

Physiologically-based pharmacokinetic (PBPK) models are progressively being used to relate tissue physiology, anatomy, and biochemistry in the prediction of tissue concentrations vs. time profiles. The premise is to interconnect tissues of discrete volumes by blood flow to describe the transport, elimination, and pharmacologic effects in select, target organs and tissues for metabolism, excretion, sampling and activity. Physical (binding and distribution) and biochemical (Michaelis–Menten parameters, V_{max}/K_m) data are fabrics for model building. Other requisite constants include enzymatic constants for metabolism ($CL_{int,met}$ based on V_{max}/K_m), passive diffusion clearance (CL_d), and transport clearances for influx (CL_{in}) or efflux (CL_{ef}) at the basolateral membrane as well as at the apical membrane for secretion ($CL_{int,sec}$) of the eliminating organ. These, together with recent, improved estimates of tissue to plasma or blood partitioning coefficients (R_T, $C_{tissue}/C_{tissue\ blood}$, which equals $C_{tissue}/C_{venous\ blood}$) for weak bases and acids [2–4], have greatly improved the modeling outcomes.

The technique is extremely useful and uniquely pertinent to correlate in vitro and in vivo preclinical data from animals such as the mouse, rat, dog or monkey and extrapolate these to describe drug behavior in humans [5–9]. PBPK modeling/simulations have provided the basis for the identification and selection of candidates with desirable pharmacokinetic properties in drug discovery and drug development [10–13] and health risk assessment [14–20]. The technique is well suited in the appraisal of how alterations of physiological or biochemical conditions such as age [21, 22], disease states [23–26], or genetic variants in transporters, enzymes, and/or protein binding affect drug disposition [27, 28]. The recent PBPK study on the role of the anionic transporter, organic anion transporting polypeptide 1B1 (OATP1B1) related the sensitivity of the systemic pravastatin exposure to hepatic uptake, and further predicted the effects of OATP1B1 polymorphism in humans [28]. PBPK modeling has been applied to account for differences in metabolism due to enzyme abundance (for example, CYP2D6 or CYP2C9 variants) and ethnic differences in alprazolam, caffeine, chlorozoxazone, cyclosporine, midazolam, omeprazole, sildenafil, tolbutamide, triazolam, *S*-warfarin, and zolpidem metabolism [29].

Indeed, drug metabolism brings about termination of drug action in the formation of inactive metabolites. But some metabolites are active, and constitute the premise of prodrug therapy in forming active drugs. Metabolism also leads to the formation of toxic metabolites. There is a serious concern for safety considerations on the investigation of metabolites, as with metabolite-in-safety testing or MIST [30, 31], or metabolites as inhibitors of enzymes or transporters in drug–metabolite

interactions [32, 33], or when metabolites are too reactive to be monitored [34]. However, useful information may not be guaranteed by the administration of the metabolite since differences between the fates of formed vs. administered or preformed metabolites are known to exist [35, 36]. The primary purpose of this review is to summarize the utility of PBPK models in the description of drug absorption, transport, metabolism and excretion and newer aspects in PBPK model development, including the net events in transport and metabolism of a drug undergoing futile cycling with its metabolite in the liver, and integration of organ models to whole body PBPK modeling.

Uniqueness of PBPK modeling for metabolite kinetics

The pros and cons of the PBPK and compartmental modeling methods are summarized, and these readily reveal that major differences exist between compartmental and physiologically-based modeling (Table 1). The summary attests to the appropriateness and usefulness of PBPK models in the examination of metabolite kinetics. The compartmental model usually combines all the metabolite formation organs and elimination organs as the central or peripheral compartment, whereas in PBPK modeling, each organ/tissue is treated as a separate entity. In this way, the PBPK model is able to account for the amount of metabolite formed and the amount of metabolite which will not reach the systemic circulation due to immediate excretion or metabolism within the metabolite formation organ [36, 37]. Hence, elimination (metabolism and excretion) within each tissue will reduce the rate of appearance of the metabolite into the systemic circulation by the fraction that is removed, or the extraction ratio of the formed metabolite, E{mi,P} [37–39]. Only the available fraction of the amount of formed primary metabolite (F{mi,P}) is able to reach the systemic circulation (Fig. 1a). This concept, the immediate, sequential first-pass removal of the formed metabolite in situ the formation organ may be

Table 1 Differences expected of PBPK vs. compartmental models

PBPK model	Compartmental model
Accounts for sequential metabolism in organ of metabolite formation	Does not account for sequential metabolism in organ of metabolite formation
Accounts for metabolite formation and elimination within multiple designated organs	Metabolite formation is considered to be in the same, lumped, central or peripheral compartment; without sequential elimination
Considers difference in transporters for drug and metabolite	Does not consider differences in transporters for drug or metabolite
Distinguishes different effects of transport barrier for formed and preformed metabolites	Considers the same transport process for formed and preformed metabolites
Expects different kinetics between formed vs. preformed metabolite	Expects formed and preformed metabolite kinetics to be identical
Formed metabolite kinetics is modulated by drug parameters	Formed metabolite kinetics is independent of drug parameters

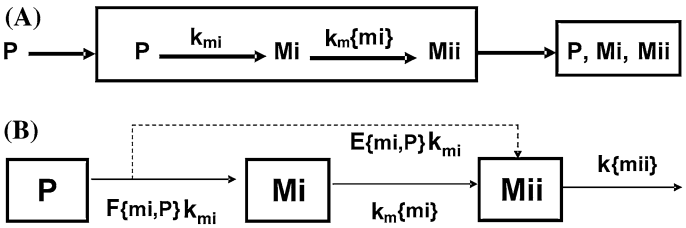

Fig. 1 Schematic depiction of sequential metabolism of a precursor drug (P) in the formation of the primary (Mi) and secondary (Mii) metabolites with rate constants, k_{mi} and $k_m\{mi\}$, respectively, within an elimination compartment (**a**), and hidden events in sequential metabolism of the primary metabolite in compartmental modeling, showing the effective formation rate constant of Mi as $F\{mi,P\}\ k_{mi}$ and not k_{mi} due to immediate removal of the formed metabolite; what disappeared yields the secondary metabolite with the effective formation rate constant, $E\{mi,P\}\ k_{mi}$; F{mi,P} and E{mi,P} are the hepatic availability and the extraction ratio of the formed metabolite, respectively (**b**)

viewed analogously to first-pass removal during drug absorption. In order to account for the lesser amount of metabolite appearing systemically, F{mi,P} is multiplied to k_{mi}, formation rate constant of the primary metabolite (Mi), to account for sequential elimination in compartmental modeling. What is lost materially should yield the secondary metabolite or that amount of Mi eliminated (Fig. 1b).

The PBPK model not only addresses the difference in transporters among tissues [35, 40] but also describes how the transport processes: passive diffusion and/or active transporters, facilitate entry of the parent drug (P) and/or the metabolite(s) into eliminating organs. Discrepant metabolite handling has been shown to occur when the metabolites display poor permeability across biological membranes [35, 41–43]. The membrane barrier can limit or even bar the metabolite from entering or leaving the tissue, thereby rendering differences in fate of the formed vs. preformed metabolite kinetics. Another unique feature of PBPK models is the incorporation of a deep/sequestered compartment to explain coupled metabolic reactions in order to account for atypical kinetic profiles of sequentially formed metabolites. Although cytosolic sulfation is the normal conjugation pathway of gentisamide, glucuronidation is the preferential sequential metabolic pathway for gentisamide which is nascently formed from salicylamide within the endoplasmic reticulum space [44]. Another example may be found in the preferential glucuronidation of estrone formed via desulfation of estrone sulfate within the same endoplasmic reticulum space, rather than the re-sulfaion of estrone in the cytosolic space [45]. A deep, intracellular compartment in liver, representing the mitochondria, has been evoked by Schwab et al. [46] for their appraisal of the glycine conjugation of benzoate in the formation of hippurate.

The PBPK model also addresses the interplay of competing pathways within the metabolite formation organ and sequential elimination of the metabolite within the same or in other downstream organs. This aspect will be addressed in the sections to follow. The various PBPK models, with the attendant differential equations, have provided solutions, defined by the various determinants, for the area under the curve (AUC) of the formed, primary metabolite Mi or AUC{mi,P}, pursuant to precursor

(P) administration. As shown in the sections to follow, the AUC{mi,P} differs from the AUC of the administered primary metabolite, AUC{pmi}. The formed metabolite area is influenced by parent drug characteristics, whereas the preformed metabolite is not, and the difference is captured in published, theoretical solutions [36, 47–50]. The discrepancy is further caused by differences in transport characteristics of the primary metabolite in each of the organs and the enzymes involved in its formation or further metabolism [36, 40, 49]. Despite these observations, administration of the preformed metabolite is often employed in metabolite-in-safety testing, with the expectation that the strategy exposes the toxicity potential of the formed metabolite arising from drug [35, 36]. However, the answer is not always positive. But when properly executed, PBPK models that utilize preformed metabolite data to enrich model parameters prove to be extremely successful in modeling of sequential metabolism [44–46] and provide accurate predictions associated with drug metabolites and in risk assessment.

PBPK models of the intestine

PBPK modeling offers a new perspective of how drug and metabolite parameters, transporters, and enzymes of the intestine modulate drug absorption and metabolite kinetics. PBPK intestinal models exist to describe absorption and intestinal elimination, based on the perfused intestine preparation [51, 52]. Various PBPK models have been used to relate data for intestinal absorption, secretion, and metabolism. The traditional model (TM) is the PBPK model that describes the intestinal tissue as a whole tissue compartment that receives blood from the superior mesenteric artery. This model describes the complement of enzymes, absorptive transporters, and ATP transporters at the apical and basolateral membrane that mediate efflux back to the lumen or circulation, respectively (Fig. 2a). The drug equilibrates across the basolateral membrane with influx (CL^{I}_{d1}) and efflux (CL^{I}_{d2}) clearances, summative terms for passive diffusion and transporter-mediated processes. However, the TM has been found to be inadequate in describing the lower extent or absence of metabolite formation following intravenous drug dosing when compared to oral dosing. The observation has prompted the development of the segregated flow model (SFM) [51], a model that presupposes that the intestinal flow to various regions to the intestine is segregated; a minor flow (5–30%, assumed as 10% of the superior mesenteric artery, Q_{SMA}, designated to equal the intestinal blood flow Q_I for simplicity) [53] perfuses the active enterocyte area which mediates absorption, metabolism and efflux, and a larger flow (90%) perfuses the remaining, nonactive serosal region, the submucosa and mucosa regions (Fig. 2b). The influx (CL^{I}_{d3}) and efflux (CL^{I}_{d4}) clearances allow equilibration of the drug between serosal blood and this serosal tissue region. The SFM is able to explain that a greater extent of metabolism occurs after oral dosing over intravenous dosing than the TM [51, 53], an observation that is distinguished otherwise as pre- and postabsorptive intestinal elimination. The concept is being adopted by others; for instance, the strategy of reduced flow is adopted by the simulation program, SimCYP® to describe intestinal metabolism of oral vs. intravenous dosing [54].

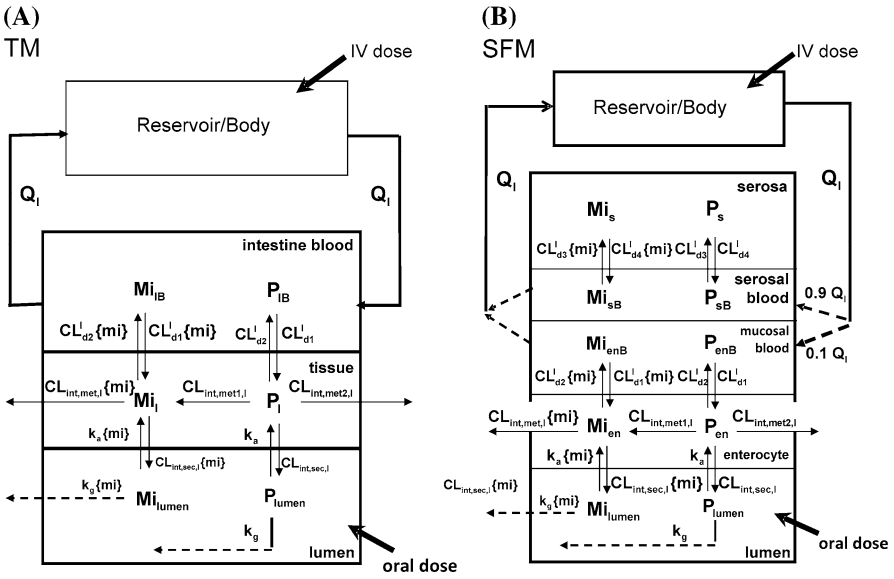

Fig. 2 Physiologically-based pharmacokinetic intestine models, the TM and the SFM that depict the intestine as the only elimination tissue as in the perfused intestine preparation. For the TM, the intestinal blood (Q_I) perfuses the entire intestinal tissue for metabolism, secretion, and absorption from the lumen. For the SFM, segregated intestinal blood flows perfuse the nonmetabolizing (90% Q_I) and enterocyte-mucosal (10% Q_I) regions. The precursor drug, P, equilibrates with those in the corresponding tissue layers with intrinsic transfer clearances CL^I_{d1} and CL^I_{d2} for TM, and as CL^I_{d1} and CL^I_{d2} between enterocyte (en) and enterocyte blood (enB), and CL^I_{d3} and CL^I_{d4} between the serosal region (s) and serosal blood (sB) for the SFM. The absorptive, metabolic, and efflux activities within the villus tips of the mucosal layer are represented by the rate constant, k_a, and metabolic ($CL_{int,met1,I}$ for Mi formation and $CL_{int,met2,I}$ for other metabolites) and secretory ($CL_{int,sec,I}$) intrinsic clearances; k_g is the rate constant that represents the loss in lumen either due to degradation or ineffective absorption. Similar processes exist for the metabolite, with the parameters classified as "{mi}" (modified from reference [40], with permission)

With the building of rate equations for the various PBPK models, AUC relationships have been developed under linear conditions upon matrix inversion [40]. Our laboratory had described these PBPK intestinal models that consider the presence of competing metabolic pathways for the drug and the metabolite within the intestine extensively (Fig. 3). In the model, the drug forms the metabolite Mi_I with $CL_{int,met1,I}$, forms other metabolites with $CL_{int,met2,I}$, and is secreted (intrinsic clearance, $CL_{int,sec,I}$), and Mi_I undergoes metabolism/secretion in the intestine with intrinsic clearances, $CL_{int,met,I}\{mi\}$ and $CL_{int,sec,I}\{mi\}$, respectively. The secretory intrinsic clearance represents the sum of both passive and carrier-mediated processes. The drug and metabolite may be absorbed from the lumen with the respective rate constants, k_a and $k_a\{mi\}$, and removed luminally by the intestine with rate constants, k_g and $k_g\{mi\}$; the fraction absorbed, F_{abs} is $k_a/(k_a + k_g)$.

With the intestine as the only metabolizing tissue in a whole body PBPK model (Fig. 3), solutions for the AUCs clearly show the influence of the binding parameters, flow, and transport and elimination intrinsic clearances of drug and metabolite on the AUC{mi,P}, and stress the importance of competing pathways

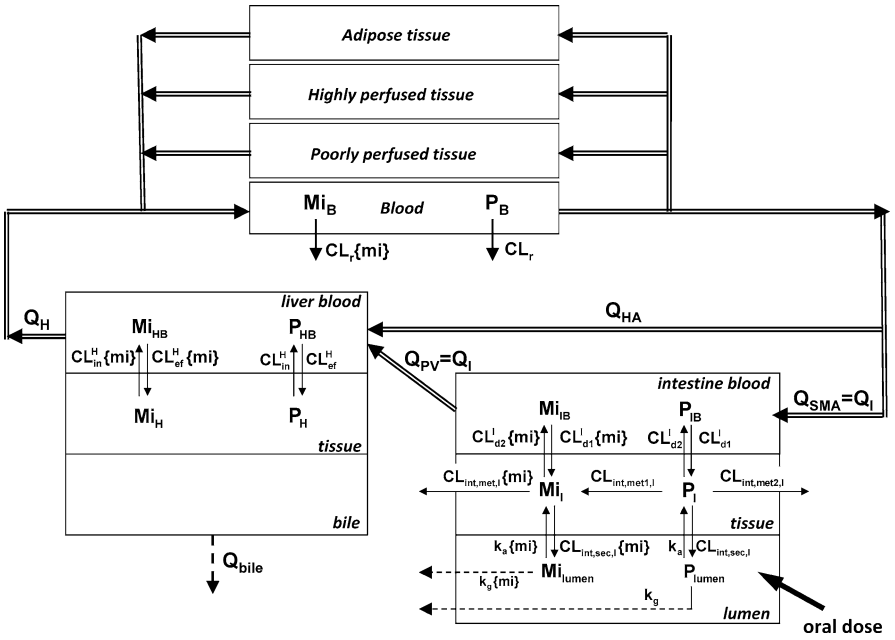

Fig. 3 A whole body PBPK model depicting the intestine as the only tissue for metabolite formation and sequential metabolism. Metabolism of drug to other metabolites also occurs in the intestine, and both drug and metabolite are secreted back to the intestinal lumen. Although the drug and metabolite distribute into the liver with CL^H_{in}, CL^H_{ef}, $CL^H_{in}\{mi\}$ and $CL^H_{ef}\{mi\}$, respectively, there is no elimination within the liver. Both the drug and metabolite is excreted by the kidneys with CL_r and $CL_r\{mi\}$, respectively. The symbols have the same meaning as in Fig. 2, and the parameters associated with the metabolite are classified as "{mi}" (modified from reference [51], with permission)

(alternate pathway of intestinal metabolism or secretion) within the formation organ and in other competing organs (renal clearance) [40]. The AUC{mi,P} resulting from intestinal metabolism only is dependent on metabolite binding, transport and eliminatory clearances, and parameters for the drug (Table 2). From the equations, the secretory intrinsic clearance is effectively reduced when there is high reabsorption of the drug ($F_{abs} \approx 1$) and metabolite ($F_{abs}\{mi\} \approx 1$), suggesting that rapid reabsorption negates secretion. The solutions for the AUC{mi,P} of the intestinally formed metabolite, Mi_I, after intravenous and oral drug administration are virtually identical when renal clearance is absent (Table 2); the only missing term is F_{abs}. Furthermore, there are clearly recognizable differences of AUC{mi,P) compared to the area after preformed metabolite administration, AUC{pmi} (solutions for AUC{pmi} is the same as those for the drug, except now the solution describes the preformed metabolite). The greatest difference occurs when there is low permeability of the metabolite [36, 40–42, 49]. These discrepancies question the legitimacy of the approach of metabolite administration to ascertain MIST [35, 36].

The relations derived from metabolite areas can enhance bioequivalence/bioavailability estimates and risk assessments. Solutions for the parent drug (AUC) and its intestinally formed primary metabolite (AUC{mi,P}) for the PBPK model

Table 2 Area under the curves for parent drug and formed metabolite under conditions of intestinal metabolism only (modified from reference [40], with permission)

Area under the curve for the parent drug after po and iv dosing

$$AUC_{po} = \frac{F_{abs}Dose_{po}Q_{PV}CL^{I}_{d2}}{CL_rQ_{PV}CL^{I}_{d2} + \left[CL_rQ_{PV} + CL^{I}_{d1}(CL_r + Q_{PV})\right]\left[CL_{int,met1,I} + CL_{int,met2,I} + (1 - F_{abs})CL_{int,sec,I}\right]}$$

$$AUC_{iv} = Dose_{iv}\frac{Q_{PV}CL^{I}_{d2} + (Q_{PV} + CL^{I}_{d1})\left[CL_{int,met1,I} + CL_{int,met2,I} + (1 - F_{abs})CL_{int,sec,I}\right]}{CL_rQ_{PV}CL^{I}_{d2} + \left[CL_rQ_{PV} + CL^{I}_{d1}(CL_r + Q_{PV})\right]\left[CL_{int,met1,I} + CL_{int,met2,I} + (1 - F_{abs})CL_{int,sec,I}\right]}$$

$$\frac{AUC_{po}/Dose_{po}}{AUC_{iv}/Dose_{iv}} = F_{sys} = F_{abs}F_I = F_{abs}\frac{Q_{PV}CL^{I}_{d2}}{Q_{PV}CL^{I}_{d2} + (Q_{PV} + CL^{I}_{d1})\left[CL_{int,met1,I} + CL_{int,met2,I} + (1 - F_{abs})CL_{int,sec,I}\right]}$$

(a) AUC for formed metabolite, when drug is renally excreted with clearance, CL_r

$$AUC_{po}\{mi,P\} = \frac{F_{abs}Dose_{po}CL_{int,met1,I}\left[CL^{I}_{d1}(CL_r + Q_{PV}) + CL_rQ_{PV}\right]}{CL_rQ_{PV}CL^{I}_{d2} + \left[CL_rQ_{PV} + CL^{I}_{d1}(CL_r + Q_{PV})\right]\left[CL_{int,met1,I} + CL_{int,met2,I} + (1 - F_{abs})CL_{int,sec,I}\right]} \times \frac{Q_{PV}CL^{I}_{d2}\{mi\}}{CL_r\{mi\}Q_{PV}CL^{I}_{d2}\{mi\} + \left[CL_r\{mi\}Q_{PV} + CL^{I}_{d1}\{mi\}(CL_r\{mi\} + Q_{PV})\right]\left[CL_{int,met,I}\{mi\} + (1 - F_{abs}\{mi\})CL_{int,sec,I}\{mi\}\right]}$$

$$AUC_{iv}\{mi,P\} = \frac{Dose_{iv}CL_{int,met1,I}Q_{pv}CL^{I}_{d1}}{CL_rQ_{PV}CL^{I}_{d2} + \left[CL_rQ_{PV} + CL^{I}_{d1}(CL_r + Q_{PV})\right]\left[CL_{int,met1,I} + CL_{int,met2,I} + (1 - F_{abs})CL_{int,sec,I}\right]} \times \frac{Q_{pv}CL^{I}_{d2}\{mi\}}{CL_r\{mi\}Q_{PV}CL^{I}_{d2}\{mi\} + \left[CL_r\{mi\}Q_{PV} + CL^{I}_{d1}\{mi\}(CL_r\{mi\} + Q_{PV})\right]\left[CL_{int,met,I}\{mi\} + (1 - F_{abs}\{mi\})CL_{int,sec,I}\{mi\}\right]}$$

$$\frac{AUC_{po}\{mi,P\}/Dose_{po}}{AUC_{iv}\{mi,P\}/Dose_{iv}} = F_{abs}\frac{\left[CL^{I}_{d1}(CL_r + Q_{PV}) + CL_rQ_{PV}\right]}{Q_{PV}CL^{I}_{d1}} = F_{abs}\left[1 + \frac{CL_r(CL^{I}_{d1} + Q_{PV})}{Q_{PV}CL^{I}_{d1}}\right]$$

(b) AUC for formed metabolite, when $CL_r = 0$

$$AUC_{po}\{mi,P\} = \frac{F_{abs}Dose_{po}CL_{int,met1,I}CL^{I}_{d2}\{mi\}}{CL^{I}_{d1}\{mi\}\left[CL_{int,met1,I} + CL_{int,met2,I} + (1 - F_{abs})CL_{int,sec,I}\right]\left[CL_{int,met,I}\{mi\} + (1 - F_{abs})CL_{int,sec,I}\{mi\}\right]}$$

$$AUC_{iv}\{mi,P\} = \frac{Dose_{iv}CL_{int,met1,I}CL^{I}_{d2}\{mi\}}{CL^{I}_{d1}\{mi\}\left[CL_{int,met,I}\{mi\} + (1 - F_{abs})CL_{int,sec,I}\{mi\}\right]\left[CL_{int,met1,I} + CL_{int,met2,I} + (1 - F_{abs})CL_{int,sec,I}\right]}$$

$$\frac{AUC_{po}\{mi,P\}/Dose_{po}}{AUC_{iv}\{mi,P\}/Dose_{iv}} = F_{abs}$$

approach [40] clearly show that the AUC_{po}/AUC_{iv} of the drug yields the systemic bioavailability (F_{sys} or $F_{abs}F_I$), whereas the ratio of the metabolite areas or $AUC\{mi,P\}_{po}/AUC\{mi,P\}_{iv}$ after po and iv drug dosing yields the fraction of dose absorbed (F_{abs}) when renal clearance of drug is absent ($CL_r = 0$) (Table 2) [40]. The quotient of these area ratios (drug/metabolite) yields the intestinal availability of the drug, F_I, when the intestine is the only eliminating organ [40]. In both instances, regardless of whether the drug is renally excreted or not ($CL_r > 0$ or $= 0$), the metabolite/drug area ratio after po and iv dosing of drug—$[AUC_{po}\{mi,P\}/AUC_{po}]/[AUC_{iv}\{mi,P\}/AUC_{iv}]$—equals $\frac{\left[1+\frac{CL_r(CL^I_{dl}+Q_{PV})}{Q_{PV}CL^I_{dl}}\right]}{F_I}$ and $\frac{1}{F_I}$, respectively, and exceed unity [40], indicative of first-pass intestinal metabolism.

Extensions of the TM and SFM have been developed, with the recognition that there are segmental differences in distribution of enzymes and transporters [53, 55]. Expansion of the tissue compartment into three segments (duodenal, jejunal, and ileal) and their corresponding flows for the enterocyte and serosal regions allows an examination of the effects of different enzymes and transporters which are heterogeneously distributed [55]. The impact of proximal distribution of CYP3A and not of P-gp (distal) as the strategic factor that affects drug bioavailability has been described [55].

PBPK models of the liver

The PBPK model of the liver and the body/reservoir based on the liver organ only (Fig. 4) has greatly enriched the development of conceptual frameworks of hepatic drug clearances [1, 35, 37, 40, 56]. The reservoir (blood compartment) and liver tissue are interconnected by the hepatic blood flow rate, Q_H. Rate equations have been developed for the compartments: reservoir (R), liver blood (HB), liver (H) and bile compartments. The unbound fraction, normally described as the unbound fraction in blood, f_u, corrects for the binding to plasma and/or red blood cells. Q_H and Q_{bile} denote the total hepatic blood flow and bile flow rates, respectively. When the liver is the only metabolite formation organ, the split flow (Q_{HA} and Q_{PV}) can be presented summatively as Q_H. The model allows for both passive and transporter-mediated processes at the sinusoidal (basolateral) membrane to be expressed collectively as the influx (CL^H_{in}) and efflux (CL^H_{ef}) clearances to denote the entry and exit transfer clearances of the precursor drug (P) or of the hepatically formed primary metabolite or Mi_H. The formation intrinsic clearance of the metabolite ($CL_{int,met1,H}$) as well as for other metabolites ($CL_{int,met2,H}$) and the secretory ($CL_{int,sec,H}$) intrinsic clearance constitute the total hepatic drug intrinsic clearance ($CL_{int,H}$), and Mi_H may be further metabolized in the liver (with intrinsic clearance, $CL_{int,met,H}\{mi\}$) or excreted into bile (with intrinsic clearance, $CL_{int,sec,H}\{mi\}$). In absence of other drug eliminating organs, AUC{mi,P} solutions for the liver as an eliminating organ in isolation (Fig. 4) or as the only metabolic organ in a whole body PBPK (Fig. 5) are identical (Table 3). Within this whole body PBPK, the liver is the only metabolizing organ; there is no contribution by the intestine to drug metabolism or excretion (Fig. 5).

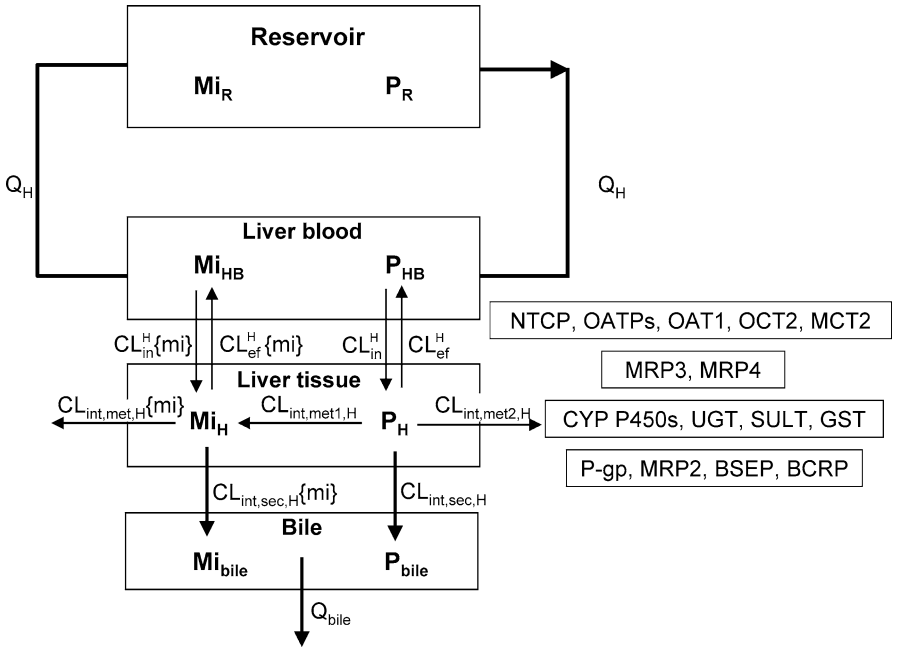

Fig. 4 Physiologically-based pharmacokinetic model of the liver as the only elimination organ. The model is divided into four compartments: the reservoir (R), liver blood (HB), liver tissue (H) and bile compartment (bile). The influx (CL^H_{in}) and efflux (CL^H_{ef}) clearances for drug at the basolateral membrane control the entry and exit of the parent drug (P) or metabolite (Mi) (classified as {mi}) between blood and liver tissue. Only the unbound drug or metabolite undergoes transport and metabolism and is considered in the rate equations, though these are not shown graphically for simplification. Metabolism occurs with the metabolite formation intrinsic clearance, $CL_{int,met1,H}$ for the assigned metabolite Mi_H, or $CL_{int,met2,H}$ for alternate metabolites; the drug also undergoes biliary excretion, with the secretory intrinsic clearance, $CL_{int,sec,H}$. Hepatic blood flow rate and bile flow rate are denoted by Q_H and Q_{bile}, respectively. Note the panels of transporters for influx, enzymes for metabolism, and transporters for biliary excretion

These solutions for AUC{mi,P} show that they are defined by precursor parameters such as $CL_{int,met,H}$ and $CL_{int,sec,H}$, regardless of hepatic transfer clearances (Table 3). Differences are immediately recognizable from the solutions for AUC{mi,P} and AUC{pmi} when the liver is the only metabolite formation organ. The AUC{pmi} is only dependent on metabolite parameters (as in solutions for drug, now for pmi; Table 3). When the liver is the only elimination organ ($CL_r = 0$), the dose corrected $AUC_{po}\{mi,P\}/AUC_{iv}\{mi,P\}$ ratio yields F_{abs}, the fraction of dose absorbed to enter the intestinal tissue (Table 3), but this ratio is influenced by CL_r when the drug is also renally cleared. When $CL_r = 0$, division of the $AUC_{po}\{mi,P\}/AUC_{iv}\{mi,P\}$ ratio into AUC_{po}/AUC_{iv} yields the hepatic availability, F_H (Table 3). In either instances, regardless of whether the drug is renally excreted or not ($CL_r > 0$ or $= 0$), the metabolite/drug area ratio after po and iv dosing of drug—$[AUC_{po}\{mi,P\}/AUC_{po}]/[AUC_{iv}\{mi,P\}/AUC_{iv}]$—equals $\frac{1+CL_r/Q_H}{F_H}$

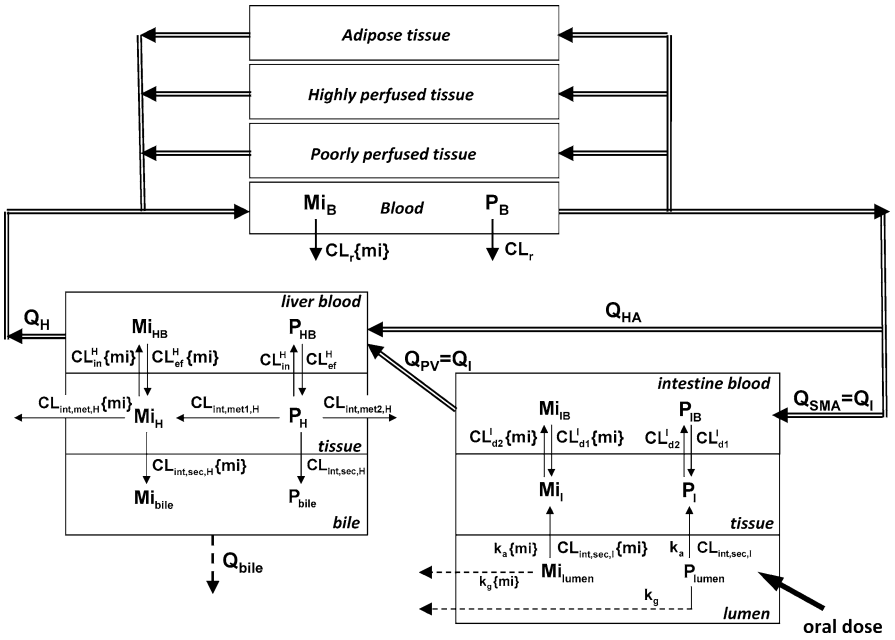

Fig. 5 A whole body PBPK model depicting the liver as the only tissue for metabolite formation and sequential metabolism. The drug is metabolized to other metabolites; both drug and metabolite are secreted by the liver. The drug and metabolite distribute into the intestinal tissue, though no elimination occurs within this tissue, and both the drug and metabolite are excreted by the kidneys. The *symbols* have been defined in Figs. 2, 3, 4 (modified from reference [51], with permission)

and $\frac{1}{F_H}$, respectively, and exceeds unity [40], indicative of first-pass liver metabolism. Acinar heterogeneity of enzymes and transporters further modifies the kinetics of drugs and metabolites [50, 57–59].

Liver PBPK model for futile cycling

Although metabolism is normally considered as an irreversible process, the metabolite often re-forms the parent drug and undergoes "reversible metabolism" or "futile cycling". The interconversion between the parent drug and its metabolite may exist for phase I [60, 61] metabolites between oxidative and reductive reactions or phase II metabolites for deconjugation and reconjugation [62–65], and acinar heterogeneity of the enzymes and transporters further modifies the kinetics of futile cycling [45, 66].

There has been some development in PBPK modeling to consider futile cycling kinetics. For modeling purposes, we consider the scenario that the precursor drug is metabolized to its interconversion metabolite by the metabolite formation intrinsic clearance, $CL^{P\rightarrow Mi}_{int,met,H}$, and to other metabolites by the metabolic intrinsic clearance,

Table 3 Area under the curves for parent drug and formed metabolite under conditions of hepatic metabolism only, with and without renal drug excretion (modified from reference [40], with permission)

Area under the curve for the parent drug after po and iv dosing

$$AUC_{po} = \frac{F_{abs}Dose_{po}Q_H(CL_{ef}^H + CL_{int,H})}{CL_rQ_H(CL_{ef}^H + CL_{int,H}) + CL_{in}^H CL_{int,H}(CL_r + Q_H)}$$

$$AUC_{iv} = Dose_{iv}\frac{Q_H(CL_{ef}^H + CL_{int,H}) + CL_{in}^H CL_{int,H}}{CL_rQ_H(CL_{ef}^H + CL_{int,H}) + CL_{in}^H CL_{int,H}(CL_r + Q_H)}$$

$$\frac{AUC_{po}Dose_{po}}{AUC_{iv}Dose_{iv}} = F_{sys} = F_{abs}F_H = F_{abs}\frac{Q_H(CL_{ef}^H + CL_{int,H})}{Q_H(CL_{ef}^H + CL_{int,H}) + CL_{in}^H CL_{int,H}}$$

(a) AUC for formed metabolite, when drug is renally excreted with clearance, CL_r

$$AUC_{po}\{mi,P\} = \frac{F_{abs}Dose_{po}Q_H CL_{in}^H CL_{int,met1,H}(CL_r + Q_H)}{CL_rQ_H(CL_{ef}^H + CL_{int,H}) + CL_{in}^H CL_{int,H}(CL_r + Q_H)} \times \frac{CL_{ef}^H\{mi\}}{CL_r\{mi\}Q_H(CL_{ef}^H\{mi\} + CL_{int,H}\{mi\}) + CL_{in}^H\{mi\}CL_{int,H}\{mi\}(CL_r\{mi\} + Q_H)}$$

$$AUC_{iv}\{mi,P\} = \frac{Dose_{iv}Q_H CL_{in}^H CL_{int,met1,H}}{CL_rQ_H(CL_{ef}^H + CL_{int,H}) + CL_{in}^H CL_{int,H}(CL_r + Q_H)} \times \frac{Q_H CL_{ef}^H\{mi\}}{CL_r\{mi\}Q_H(CL_{ef}^H\{mi\} + CL_{int,H}\{mi\}) + CL_{in}^H\{mi\}CL_{int,H}\{mi\}(CL_r\{mi\} + Q_H)}$$

$$\frac{AUC_{po}\{mi,P\}/Dose_{po}}{AUC_{iv}\{mi,P\}/Dose_{iv}} = \frac{F_{abs}(Q_H + CL_r)}{Q_H} = F_{abs}(1 + \frac{CL_r}{Q_H})$$

(b) AUC for formed metabolite, when $CL_r = 0$

$$AUC_{po}\{mi,P\} = \frac{F_{abs}Dose_{po}CL_{int,met1,H}CL_{ef}^H\{mi\}}{CL_{in}^H\{mi\}CL_{int,H}CL_{int,H}\{mi\}}$$

$$AUC_{iv}\{mi,P\} = \frac{Dose_{iv}CL_{int,met1,H}CL_{ef}^H\{mi\}}{CL_{in}^H\{mi\}CL_{int,H}CL_{int,H}\{mi\}}$$

$$\frac{AUC_{po}\{mi,P\}/Dose_{po}}{AUC_{iv}\{mi,P\}/Dose_{iv}} = F_{abs}$$

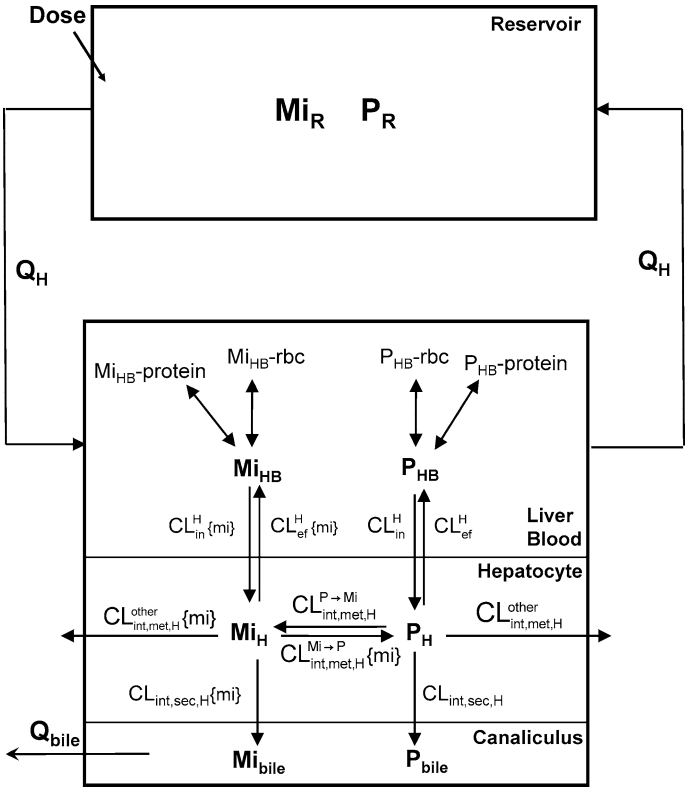

Fig. 6 Schematic depiction of futile cycling between a precursor, P, and its metabolite, Mi. The forward and backward, interconversion intrinsic clearances are $CL^{P\to Mi}_{int,met,H}$ and $CL^{Mi\to P}_{int,met,H}\{mi\}$, respectively. Both the drug and metabolite may form other metabolites and are excreted into bile. There is red cell and protein binding of the parent drug and metabolite, shown in liver blood, and also occurs in reservoir blood (modified from Ref. [67], with permission)

$CL^{other}_{int,met,H}$. Similarly, the interconversion metabolite re-forms the precursor drug with the metabolic intrinsic clearance for the metabolite, $CL^{Mi\to P}_{int,met,H}\{mi\}$, or forms other secondary metabolites with the intrinsic clearance, $CL^{other}_{int,met,H}\{mi\}$. Both the precursor and metabolite in the hepatocyte may be effluxed back to the sinusoid with CL^{H}_{ef} and $CL^{H}_{ef}\{mi\}$, respectively, or are excreted biliarily with $CL_{int,sec,H}$ and $CL_{int,sec,H}\{mi\}$, respectively (Fig. 6). The solutions for the AUC based on a simple liver model for futile cycling have been solved [67]. It becomes clear that the areas under the curve for drug (AUC_R) and for the metabolite ($AUC_R\{mi,P\}$) undergoing futile cycling are exceedingly similar to those in absence of futile cycling, with the exception of two new terms: ef''_m and ef'_m that effectively modify the metabolic intrinsic clearances of the forward ($CL^{P\to Mi}_{int,met,H}$) and backward ($CL^{Mi\to P}_{int,met,H}\{mi\}$) processes in futile cycling (Table 4). The fraction, ef''_m or

Table 4 Analytical solutions for the area of the curve from time 0 to infinity for the parent drug (AUC_R and AUC_H) and formed metabolite ($AUC_R\{mi,P\}$ and $AUC_H\{mi,P\}$) in reservoir and liver tissue, respectively, and cumulative amounts of biliarily excreted parent drug ($A_{e,bile,\infty}$) and metabolite ($A_{e,bile,\infty}\{mi,P\}$) for a drug–metabolite pair in absence ($CL^{Mi\to P}_{int,met,H}\{mi\} = 0$) and presence ($CL^{Mi\to P}_{int,met,H}\{mi\} > 0$) of futile cycling (modified from Ref. [67], with permission)

Terms	Solutions
AUC_R	$\dfrac{\text{Dose}\left[Q_H(CL^H_{ef} + CL_{int,sec,H} + ef''_m\ CL^{P\to Mi}_{int,met,H} + CL^{other}_{int,met,H}) + f_B CL^H_{in}(CL_{int,sec,H} + ef''_m\ CL^{P\to Mi}_{int,met,H} + CL^{other}_{int,met,H})\right]}{Q_H f_B CL^H_{in}(CL_{int,sec,H} + ef''_m\ CL^{P\to Mi}_{int,met,H} + CL^{other}_{int,met,H})}$
AUC_H	$\dfrac{\text{Dose}}{f_H(CL_{int,sec,H} + CL^{other}_{int,met,H} + ef''_m\ CL^{P\to Mi}_{int,met,H})}$
$A_{e,bile,\infty}$	$\dfrac{\text{Dose}\ CL_{int,sec,H}}{(CL_{int,sec,H} + CL^{other}_{int,met,H} + ef''_m\ CL^{P\to Mi}_{int,met,H})}$
$AUC_R\{mi,P\}$	$\dfrac{\text{Dose}\ CL^H_{ef}\{mi\}CL^{P\to Mi}_{int,met,H}}{f_B\{mi\}CL^H_{in}\{mi\}(CL_{int,sec,H} + CL^{P\to Mi}_{int,met,H} + CL^{other}_{int,met,H})(CL_{int,sec,H}\{mi\} + ef'_m\ CL^{Mi\to P}_{int,met,H}\{mi\} + CL^{other}_{int,met,H}\{mi\})}$
$AUC_H\{mi,P\}$	$\dfrac{\text{Dose}\ CL^{P\to Mi}_{int,met,H}}{f_H\{mi\}(CL_{int,sec,H} + CL^{P\to Mi}_{int,met,H} + CL^{other}_{int,met,H})(CL_{int,sec,H}\{mi\} + ef'_m\ CL^{Mi\to P}_{int,met,H}\{mi\} + CL^{other}_{int,met,H}\{mi\})}$
$A_{e,bile,\infty}\{mi,P\}$	$\dfrac{\text{Dose}\ CL^{P\to Mi}_{int,met,H}CL_{int,sec,H}\{mi\}}{(CL_{int,sec,H} + CL^{P\to Mi}_{int,met,H} + CL^{other}_{int,met,H})(CL_{int,sec}\{mi\} + ef'_m\ CL^{Mi\to P}_{int,met,H}\{mi\} + CL^{other}_{int,met,H}\{mi\})}$

In absence of futile cycling, $CL^{Mi\to P}_{int,met,H}\{mi\} = 0$, rendering $ef''_m = 1$; in presence of futile cycling, $CL^{Mi\to P}_{int,met,H}\{mi\} > 0$, rendering $0 < ef''_m < 1$

$\frac{CL_{int,sec,H}\{mi\}+CL^{other}_{int,met,H}\{mi\}}{CL_{int,sec,H}\{mi\}+CL^{Mi\to P}_{int,met,H}\{mi\}+CL^{other}_{int,met,H}\{mi\}}$, is the effective coefficient for metabolite formation or the fraction that reduces the intrinsic clearance for metabolite formation, $CL^{P\to Mi}_{int,met,H}$. The second term, ef'_m or $\frac{CL_{int,sec,H}+CL^{other}_{int,met,H}}{CL_{int,sec,H}+CL^{P\to Mi}_{int,met,H}+CL^{other}_{int,met,H}}$, is the effective recycling coefficient that reduces the metabolic intrinsic clearance of the metabolite in re-forming the precursor, $CL^{Mi\to P}_{int,met,H}\{mi\}$ (Table 4). The value of ef''_m is less than unity, and a low ef''_m value suggests a pronounced effect of futile cycling on precursor disposition. With futile cycling, ef'_m modifies $CL^{Mi\to P}_{int,met,H}\{mi\}$ by appearing as a product, thus yielding a lower AUC{mi,P} with a high ef'_m. When futile cycling is absent ($CL^{Mi\to P}_{int,met,H}\{mi\} = 0$), ef''_m equals unity.

The AUC for the precursor in reservoir, AUC_R, is highly influenced by the intrinsic clearances of the precursor for basolateral influx (CL^H_{in}) and efflux (CL^H_{ef}), the metabolic ($CL^{P\to Mi}_{int,met,H}$and $CL^{other}_{int,met,H}$) and secretory ($CL_{int,sec,H}$) intrinsic clearances as well as ef''_m. Analogously, the AUC of the drug in liver, AUC_H, is affected by the unbound fraction in liver, f_H, and both this and the cumulative excretion of the precursor drug ($A_{e,bile,\infty}$) are affected by ef''_m when futile cycling occurs (Table 4). The AUC for the formed metabolite in the reservoir, AUC_R\{mi,P\} is dependent on parent drug and additionally, those for metabolite handling ($CL^H_{in}\{mi\}$, $CL^H_{ef}\{mi\}$, $CL_{int,sec,H}\{mi\}$, $CL^{Mi\to P}_{int,met,H}\{mi\}$), metabolite formation ($CL^{P\to Mi}_{int,met,H}$), secretory intrinsic ($CL_{int,sec,H}$) clearances, and the metabolic intrinsic clearance for alternate metabolism ($CL^{other}_{int,met,H}$). Again, the AUC for metabolite in liver or AUC_H\{mi,P\}, and the cumulative excretion of the metabolite ($A_{e,bile,\infty}\{mi,P\}$) are affected by ef'_m when futile cycling occurs. These areas allow the apparent total ($CL_{liver,tot}$) and excretory ($CL_{liver,ex}$) clearances, estimated as Dose/AUC_R and $A_{e,bile,\infty}/AUC_R$, respectively, with the metabolic clearance ($CL_{liver,met}$) being estimated by difference ($CL_{liver,tot} - CL_{liver,ex}$) (Table 5). Notably, ef''_m appears as a product with $CL^{P\to Mi}_{int,met,H}$ in the solutions of the apparent clearances (Table 5). These relations are much simplified when the transmembrane barrier does not exist, namely, $CL^H_{in} = CL^H_{ef} \gg Q_H$ and $CL_{int,sec,H}$, $ef''_m CL^{P\to Mi}_{int,met,H}$ and $CL^{other}_{int,met,H}$ (Table 5).

To understand how futile cycling kinetics is affected by the transporter function for the excretion of the metabolite and drug, simulations have been conducted to examine the profiles in the liver (AUC_H and AUC_H\{mi,P\}) when the transporter activity of MRP2 for the parent drug and metabolite is reduced, using $E_2$17G and $E_2$3S17G in the perfused rat liver preparation as examples [67]. The extent of change is dramatic when both the precursor and metabolite secretory transporter activities are both diminished (Fig. 7a, b). With loss of biliary secretory function, the net metabolic clearance (forward reaction) is decreased due to increased futile cycling, leading to an apparent decrease in the net metabolic and total clearances for the precursor (Fig. 7c).

Table 5 Analytical solutions for metabolic ($CL_{liver,met}$), excretory ($CL_{liver,ex}$), and total ($CL_{liver,tot}$) liver clearances in the presence of futile cycling (modified from Ref. [67], with permission)

Clearances	With barrier	Without barrier $CL_{in}^{H} = CL_{ef}^{H} \gg Q_H \gg CL_{int,sec,H}, ef_m'' CL_{int,met,H}^{P\to Mi}$ & $CL_{int,met,H}^{other}$
$CL_{liver,ex}$	$\dfrac{Q_H f_B CL_{in}^{H} CL_{int,sec,H}}{\left[Q_H(CL_{ef}^{H} + CL_{int,sec,H} + ef_m'' CL_{int,met,H}^{P\to Mi} + CL_{int,met,H}^{other}) + f_B CL_{in}^{H}(CL_{int,sec,H} + ef_m'' CL_{int,met,H}^{P\to Mi} + CL_{int,met,H}^{other})\right]}$	$\dfrac{Q_H f_B CL_{int,sec,H}}{\left[Q_H + f_B(CL_{int,sec,H} + ef_m'' CL_{int,met}^{P\to Mi} + CL_{int,met}^{other})\right]}$
$CL_{liver,met}$	$\dfrac{Q_H f_B CL_{in}^{H}(ef_m'' CL_{int,met,H}^{P\to Mi} + CL_{int,met,H}^{other})}{\left[Q_H(CL_{ef}^{H} + CL_{int,sec,H} + ef_m'' CL_{int,met,H}^{P\to Mi} + CL_{int,met,H}^{other}) + f_B CL_{in}^{H}(CL_{int,sec,H} + ef_m'' CL_{int,met,H}^{P\to Mi} + CL_{int,met,H}^{other})\right]}$	$\dfrac{Q_H f_B(ef_m'' CL_{int,met,H}^{P\to Mi} + CL_{int,met,H}^{other})}{\left[Q_H + f_B(CL_{int,sec,H} + ef_m'' CL_{int,met}^{P\to Mi} + CL_{int,met,H}^{other})\right]}$
$CL_{liver,tot}$	$\dfrac{Q_H f_B CL_{in}^{H}(CL_{int,sec,H} + ef_m'' CL_{int,met,H}^{P\to Mi} + CL_{int,met,H}^{other})}{\left[Q_H(CL_{ef}^{H} + CL_{int,sec,H} + ef_m'' CL_{int,met,H}^{P\to Mi} + CL_{int,met,H}^{other}) + f_B CL_{in}^{H}(CL_{int,sec,H} + ef_m'' CL_{int,met,H}^{P\to Mi} + CL_{int,met,H}^{other})\right]}$	$\dfrac{Q_H f_B(CL_{int,sec,H} + ef_m'' CL_{int,met,H}^{P\to Mi} + CL_{int,met,H}^{other})}{\left[Q_H + f_B(CL_{int,sec,H} + ef_m'' CL_{int,met}^{P\to Mi} + CL_{int,met,H}^{other})\right]}$
$CL_{liver,tot}$	$\dfrac{Q_H f_B CL_{in}^{H}(CL_{int,sec,H} + ef_m'' CL_{int,met,H}^{P\to Mi} + CL_{int,met,H}^{other})}{\left[Q_H(CL_{ef}^{H} + CL_{int,sec,H} + ef_m'' CL_{int,met,H}^{P\to Mi} + CL_{int,met,H}^{other}) + f_B CL_{in}^{H}(CL_{int,sec,H} + ef_m'' CL_{int,met,H}^{P\to Mi} + CL_{int,met,H}^{other})\right]}$	$\dfrac{Q_H f_B(CL_{int,sec,H} + ef_m'' CL_{int,met,H}^{P\to Mi} + CL_{int,met,H}^{other})}{\left[Q_H + f_B(CL_{int,sec,H} + ef_m'' CL_{int,met}^{P\to Mi} + CL_{int,met,H}^{other})\right]}$

The solutions for the total hepatic ($CL_{liver,tot}$) and the excretory ($CL_{liver,ex}$) clearances were obtained by Dose/AUC_R and $A_{e,bile,\infty}/AUC_R$, respectively. The metabolic clearance was estimated by the difference of $CL_{liver,tot}$ and $CL_{liver,ex}$

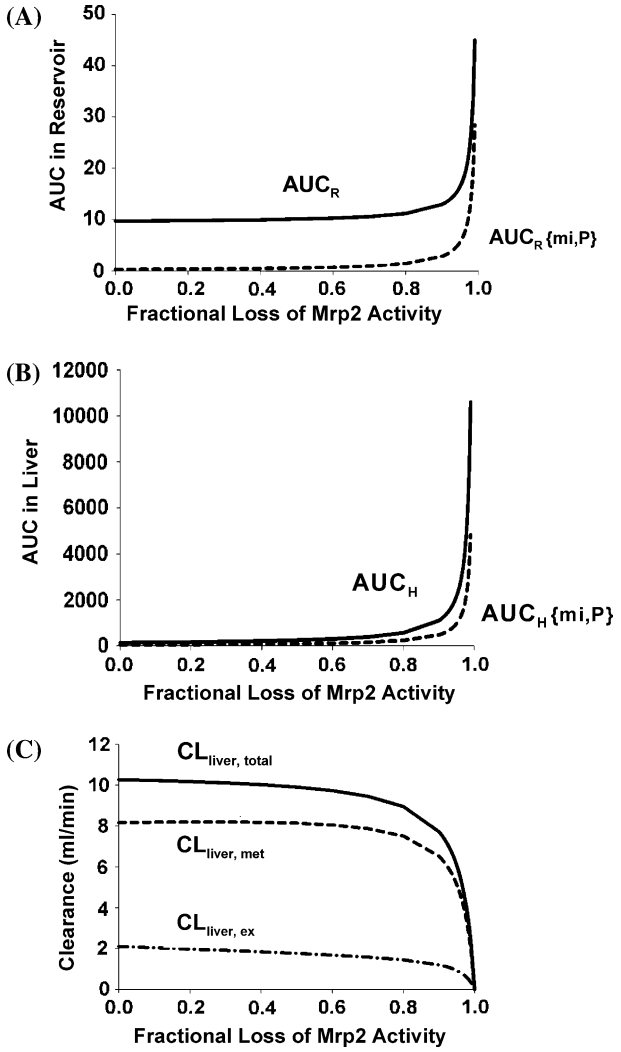

Fig. 7 Profiles of AUCs for the drug, AUC_R (*solid line*) and metabolite $AUC_R\{mi,P\}$ (*dotted line*), in reservoir (**a**), and AUC_H (*solid line*) and $AUC_H\{mi,P\}$(*dotted line*) in liver (**b**), when the secretory function of Mrp2 is reduced (based on relations shown in Table 4). The example was simulated based on perfusion data for Wistar and TR^- liver preparations for $E_2$17G that undergoes futile cycling with its metabolite $E_2$3S17G, both of which are excreted by Mrp2. The metabolic (*dotted line*), excretory (*dashed with dotted line*), and total (*solid line*) drug hepatic clearances with reduction/loss of Mrp2 activities are shown, based on relations shown in Table 5 (**c**) (from reference [67], with permission)

Intestine and liver PBPK models

It is well known that metabolism occurs in both the intestine and liver. A drug may form distinctively different metabolites Mi_I and Mii_H within the intestine and liver, respectively (Fig. 8). Each metabolite may be metabolized and/or excreted within its organ of formation and not in other tissues, namely, Mi_I formed from the

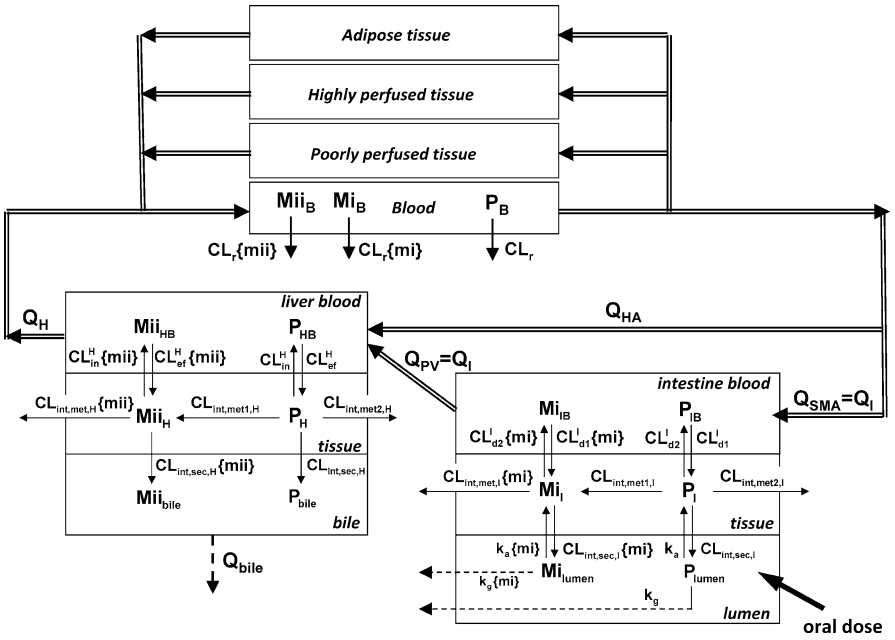

Fig. 8 A whole body PBPK model depicting the intestine and liver as tissues for metabolite formation and sequential metabolism. Separate metabolites may be formed by the intestine and liver, respectively, and the formed metabolites can distribute into the alternate organ but is only eliminated by the formation organ and kidney. Or, the same primary metabolite is formed in both liver and intestine. Both the drug and metabolite are excreted by the kidneys (modified from reference [51], with permission)

intestine may enter the liver but not for further processing, and the same applies to the hepatically formed Mii_H. These AUC solutions are very complex, and the ratio of AUC_{po}/AUC_{iv} or F_{sys} is $F_{abs}F_IF_H$ (Table 6), with the F_I and F_H terms identical to those solved for the intestine and liver (as in Tables 2 and 3). The metabolite areas after oral and intravenous drug dosing are clearly influenced by all of the drug and metabolite parameters. $AUC_{po}\{mi,P\}/AUC_{iv}\{mi,P\}$ for the intestinally formed metabolite, Mi_I, is affected by F_{abs}, the separate liver blood flows for the portal vein (Q_{PV}) and the hepatic artery (Q_{HA}), and expectedly, also by the hepatic intrinsic clearances, the drug influx intrinsic clearances in liver (CL^H_{in} and CL^H_{ef}) and intestine (CL^I_{d1} and CL^I_{d2}), as well as the renal clearance (CL_r). For this hepatically formed metabolite, Mii_H, $AUC_{po}\{mii,P\}/AUC_{iv}\{mii,P\}$ is modulated by F_{abs}, Q_{PV}, Q_{HA}, the intrinsic metabolic clearance of the intestine, CL^I_{d1}, CL^I_{d2}, CL^H_{in} and CL^H_{ef} as well as CL_r. The solutions for the AUC_{po} and AUC_{iv} are found to be simplified considerably if $CL_r = 0$, as are the $AUC_{po}\{mii,P\}/AUC_{iv}\{mii,P\}$ and $AUC_{po}\{mii,P\}/AUC_{iv}\{mii,P\}$ ratios (Table 6).

The more common occurrence is when the same metabolite M_i is formed in both the intestine and the liver. The intestinally formed metabolite may enter the liver for further processing; the same applies to the hepatically formed metabolite, which can enter the intestine for further sequential processing. In this scenario, solutions for the drug AUCs and metabolite (po and iv) are too bulky to be simplified into

Table 6 Area under the curves for parent drug and formed metabolite under conditions of intestinal and liver metabolism, each forming a different metabolite, Mi_I in intestine and Mii_H in liver, with and without renal drug excretion (modified from reference [40], with permission)

$$\frac{AUC_{po}/Dose_{po}}{AUC_{iv}/Dose_{iv}} = F_{sys} = F_{abs}F_I\ F_H = F_{abs}\left[\frac{Q_{PV}CL^I_{d2}}{Q_{PV}CL^I_{d2} + (Q_{PV} + CL^I_{d1})[CL^I_{int,met1,I} + CL^I_{int,met2,I} + CL^I_{int,sec,I}(1 - F_{abs})]}\right]\left[\frac{Q_H(CL^H_{ef} + CL_{int,H})}{Q_H(CL^H_{ef} + CL_{int,H}) + CL^H_{in}CL_{int,H}}\right]$$

(a) AUC for formed metabolites in intestine and liver, when drug is renally excreted with clearance, CL_r

For the intestinally formed metabolite, Mi_I

$$\frac{AUC_{po}\{mi,P\}\ /Dose_{po}}{AUC_{iv}\{mi,P\}\ /Dose_{iv}} = F_{abs}\frac{CL^H_{ef}\left(CL^I_{d1} + Q_{PV}\right)(CL_r + Q_H)CL_{int,H} + Q_H\left[Q_{PV}(CL^I_{d1} + CL_r) + CL^I_{d1}CL_r\right](CL^H_{ef} + CL_{int,H})}{CL^I_{d1}Q_{PV}\left[CL^H_{in}CL_{int,H} + Q_H(CL^H_{ef} + CL_{int,H})\right]}$$

For the hepatically formed metabolite, Mii_H

$$\frac{AUC_{po}\{mii,P\}\ /Dose_{po}}{AUC_{iv}\{mii,P\}\ /Dose_{iv}} = F_{abs}\frac{CL^I_{d2}Q_{PV}(Q_H + CL_r)}{Q_{PV}Q_H\left[(CL^I_{d2} + CL_{int,met1,I} + CL_{int,met12,I}) + (1 - F_{abs})CL_{int,sec,I}\right] + Q_{HA}CL^I_{d1}\left[CL_{int,met1,I} + CL_{int,met12,I}) + (1 - F_{abs})CL_{int,sec,I}\right]}$$

(b) AUC for formed metabolites in intestine and liver, when $CL_r = 0$

For the intestinally formed metabolite, Mi_I

$$AUC_{po}\{mi,P\}\ = \frac{F_{abs}Dose_{po}CL_{int,met1,I}\left[CL^I_{d1}CL^H_{ef}Q_{PV} + CL_{int,H}\left[CL^H_{in}(CL^I_{d1} + Q_{PV}) + CL^I_{d1}Q_{PV}\right]\right]}{CL^H_{in}Q_{PV}CL_{int,H}CL^I_{d2} + \left[CL_{int,met1,I} + CL_{int,met2,I} + (1 - F_{abs})CL_{int,sec,I}\right]\left[CL^I_{d1}\left[Q_{PV}(CL^H_{ef} + CL_{int,H}) + CL^H_{in}CL_{int,H}\right] + CL^H_{in}Q_{PV}CL_{int,H}\right]}$$

$$\times\frac{CL^I_{d2}\{mi\}}{CL_r\{mi\}Q_{PV}CL^I_{d2}\{mi\} + \left[CL_r\{mi\}\ Q_{PV} + CL^I_{d1}\{mi\}(CL_r\{mi\}\ + Q_{PV})\right]\left[CL_{int,met,I}\{mi\}\ + (1 - F_{abs}\{mi\})CL_{int,sec,I}\{mi\}\ \right]}$$

$$AUC_{iv}\{mi,P\}\ = \frac{Dose_{iv}CL_{int,met1,I}Q_{pv}CL^I_{d1}\left[Q_H(CL^H_{ef} + CL_{int,H}) + CL^H_{in}CL_{int,H}\right]}{CL^H_{in}Q_{PV}CL_{int,H}CL^I_{d2} + \left[CL_{int,met1,I} + CL_{int,met2,I} + (1 - F_{abs})CL_{int,sec,I}\right]\left[CL^I_{d1}\left[Q_{PV}(CL^H_{ef} + CL_{int,H}) + CL^H_{in}CL_{int,H}\right] + CL^H_{in}Q_{PV}CL_{int,H}\right]}$$

$$\times\frac{Q_{PV}CL^I_{d2}\{mi\}}{CL_r\{mi\}\ Q_{PV}CL^I_{d2}\{mi\}\ + \left[CL_r\{mi\}\ Q_{PV} + CL^I_{d1}\{mi\}\ (CL_r\{mi\}\ + Q_{PV})\right]\left[CL_{int,met,I}\{mi\}\ + (1 - F_{abs}\{mi\})CL_{int,sec,I}\{mi\}\ \right]}$$

$$\frac{AUC_{po}\{mi,P\}\ /Dose_{po}}{AUC_{iv}\{mi,P\}\ /Dose_{iv}} = F_{abs}\frac{Q_H\left[CL^I_{d1}CL^H_{ef}Q_{PV} + CL_{int,H}\left[CL^H_{in}(CL^I_{d1} + Q_{PV}) + CL^I_{d1}Q_{PV}\right]\right]}{Q_{pv}CL^I_{d1}\left[Q_H(CL^H_{ef} + CL_{int,H}) + CL^H_{in}CL_{int,H}\right]}$$

For the hepatically formed metabolite, Mii_H, only the ratio available

$$\frac{AUC_{po}\{mii,P\}/Dose_{po}}{AUC_{iv}\{mii,P\}/Dose_{iv}} = F_{abs}\frac{CL^I_{d2}Q_{PV}Q_H}{Q_{PV}Q_H\left[(CL^I_{d2} + CL_{int,met1,I} + CL_{int,met2,I}) + (1 - F_{abs})CL_{int,sec,I}\right] + Q_{HA}CL^I_{d1}\left[(CL^I_{d2} + CL_{int,met1,I} + CL_{int,met2,I}) + (1 - F_{abs})CL_{int,sec,I}\right]}$$

presentable formats. The AUC ratio of the precursor, F_{sys}, the product of F_{abs}, F_I, and F_H, is identical to that found in Table 6, regardless of whether $CL_r = 0$ or > 0. However, the $AUC_{po}\{mi,P\}$, $AUC_{iv}\{mi,P\}$ or the ratio are not in presentable forms, and, from the clusters of the solution, one can readily come to the conclusion that these are different from the former cases (intestine, liver, and intestine and liver forming different metabolites, Tables 2, 3, and 6) [40]. From the analyses involving different metabolite formation organs, the outcome of different solutions for AUC{mi,P} point to the importance of knowing which are metabolite formation organs, and which are metabolite metabolism organs, whether competing pathways exist within the same organ for both the drug and metabolite, and if competing eliminating organs are present. Since multiple metabolite formation organs are likely to be present, and since the formed, phase I metabolite usually undergoes sequential, phase II metabolism within the same or other organs, the solutions for these scenarios, though existing, are not readily presentable and are unlikely to be useful. Hence, for metabolite kinetics, it can be deduced readily that there is a need for stating the underlying assumptions on organs for drug and the metabolite formation as well as removal to expand our understanding of the factors that affect the AUC{mi,P}. Indeed, there is a need to consider not only the elimination organs but also the differential transport barriers or transporters.

PBPK metabolite modeling

While there is no simple solution for AUC{mi,P} in complicated situations, modeling and simulation of sequential metabolism data offers an alternate solution [68]. This type of approach has been performed for the sequential metabolism of codeine to morphine and morphine-3-glucuronide (M3G). The tissue partitioning coefficients, calculated according to Rodgers and Rowland [2, 3], were used to optimize parameters for transport and metabolism to correlate to literature data after the oral (po) and intravenous (iv) administration to man and the rat in PBPK models that describe the N-demethylation of codeine and glucuronidation of morphine in the intestinal and liver. It becomes apparent that the whole body PBPK model consisting of the SFM and not the TM for the intestine, together with liver metabolism and renal excretion, is superior, when ratios of $[AUC_{M3G}/AUC_{morphine}]_{po}$ and $[AUC_{M3G}/AUC_{morphine}]_{iv}$ are used as discriminators [68].

The PBPK model is well suited for investigation of metabolite toxicity and risk assessment as it gives more a more accurate estimate of the kinetics of sequential metabolism, particularly for environmental chemicals or metabolites in human or animal models [69–71], as exemplified by the trichloroethylene metabolites [72]. In a mouse PBPK model, Sweeney et al. [73] correlated the occurrence of liver carcinomas and adenomas to the hepatic exposure (AUC) of trichloroacetic acid, a toxic metabolite of perchloroethylene (a solvent commonly utilized in dry cleaning). In another example, the resultant toxic effects of the interaction between trichloroethylene (TCE) and 1,1-dichloroethylene (1,1-DCE) were well predicted using PK/PD modeling [74]. Table 7 highlights other studies in which PBPK modeling of metabolites was applied for the purpose of safety assessment.

Table 7 Metabolite kinetics with PBPK modeling

Precursor	Metabolite	References
Methylene chloride	Carbon monoxide, glucuronide	[75]
Vinyl chloride	Chloroethylene epoxide	[76, 77]
2,3,7,8-Tetrachlorodibenzo-p-dioxin (TCDD)	Glucuronides	[58]
All-trans retinoic acid	All-trans-4-oxo-retinoic acid, 13-cis-retinoic acid, glucuronide	[78]
Acrylate esters	Acrylic acid	[18, 20, 79, 80]
Methyl methacrylate	Methacrylic acid	[81]
Monoethyl and monomethyl ethers	2-Ethoxyacetic acid	[19]
Styrene	Styrene 7,8-oxide	[82]
Trichloroethylene	Chloral hydrate, trichloroacetic acid, and dichloroacetic acid	[16, 83]
Octamethylcyclotetrasiloxane	Dimethylsilanediol, methylsilanetriol	[84]
Ethylene Glycol	Glycolic acid	[85]
Atrazine	Chlorinated metabolites	[86]
Monobutyl phthalate	Monobutyl phthalate glucuronide	[87]
1,4-dioxane	Hydroxyethoxyacetic acid	[88]
Diltiazem	*N*-Desmethyldiltiazem	[89]
Coumarin and estragole	1′-Sulfooxyestragole	[90]

Conclusions

The solution for AUC{mi,P} is unique to define the circumstances for metabolite formation and the competing pathways for elimination organs. The $AUC_{po}\{mi,P\}/AUC_{iv}\{mi,P\}$ is useful for (F_{abs}) only when intestine or liver is the sole drug elimination organ; the ratio does not yield F_{sys}. For other cases, the ratio is not very useful. In the case of futile cycling, apical transporter activity modulates the AUC for drug and metabolite, and the net metabolism of drug when the metabolite and/or drug are excreted. The PBPK model, encompassing all the involved kinetic factors, is a useful tool to study transporter-enzyme interplay and to predict DDI, and can be a useful tool in risk assessment.

Acknowledgment This work was supported by the Canadian Institutes for Heath Research, MOP89850. MRD was a recipient of a Biologic Therapeutics training grant from the CIHR.

References

1. Rowland M, Benet LZ, Graham GG (1973) Clearance concepts in pharmacokinetics. J Pharmacokinet Biopharm 1:123–136
2. Rodgers T, Rowland M (2007) Mechanistic approaches to volume of distribution predictions: understanding the processes. Pharm Res 24:918–933
3. Rodgers T, Leahy D, Rowland M (2005) Physiologically based pharmacokinetic modeling 1: predicting the tissue distribution of moderate-to-strong bases. J Pharm Sci 94:1259–1276
4. Rodgers T, Rowland M (2006) Physiologically based pharmacokinetic modelling 2: predicting the tissue distribution of acids, very weak bases, neutrals and zwitterions. J Pharm Sci 95:1238–1257

5. Dedrick RL, Forrester DD, Cannon JN, el-Dareer SM, Mellett LB (1973) Pharmacokinetics of 1-beta-D-arabinofuranosylcytosine (ARA-C) deamination in several species. Biochem Pharmacol 22:2405–2417
6. Boxenbaum H, Ronfeld R (1983) Interspecies pharmacokinetic scaling and the Dedrick plots. Am J Physiol 245:R768–R775
7. Rowland M (1985) Physiologic pharmacokinetic models and interanimal species scaling. Pharmacol Ther 29:49–68
8. Kawai R, Mathew D, Tanaka C, Rowland M (1998) Physiologically based pharmacokinetics of cyclosporine A: extension to tissue distribution kinetics in rats and scale-up to human. J Pharmacol Exp Ther 287:457–468
9. Nestorov I (2003) Whole body pharmacokinetic models. Clin Pharmacokinet 42:883–908
10. Nestorov I, Aarons L, Rowland M (1998) Quantitative structure-pharmacokinetics relationships: II. A mechanistically based model to evaluate the relationship between tissue distribution parameters and compound lipophilicity. J Pharmacokinet Biopharm 26:521–545
11. Rowland M, Balant L, Peck C (2004) Physiologically based pharmacokinetics in drug development, regulatory science: a workshop report (Georgetown University, Washington, DC, May 29–30,2002. AAPS PharmSci 6:E6
12. Germani M, Crivori P, Rocchetti M, Burton PS, Wilson AG, Smith ME, Poggesi I (2007) Evaluation of a basic physiologically based pharmacokinetic model for simulating the first-time-in-animal study. Eur J Pharm Sci 31:190–201
13. Lavé T, Parrott N, Grimm HP, Fleury A, Reddy M (2007) Challenges and opportunities with modelling and simulation in drug discovery and drug development. Xenobiotica 37:1295–1310
14. Chiu WA, Barton HA, DeWoskin RS, Schlosser P, Thompson CM, Sonawane B, Lipscomb JC, Krishnan K (2007) Evaluation of physiologically based pharmacokinetic models for use in risk assessment. J Appl Toxicol 27:218–237
15. Clewell RA, Clewell HJ 3rd (2008) Development and specification of physiologically based pharmacokinetic models for use in risk assessment. Regul Toxicol Pharmacol 50:129–143
16. Dobrev ID, Andersen ME, Yang RS (2002) In silico toxicology: simulating interaction thresholds for human exposure to mixtures of trichloroethylene, tetrachloroethylene, and 1,1,1-trichloroethane. Environ Health Perspect 110:1031–1039
17. Gargas ML, Sweeney LM, Himmelstein MW, Pottenger LH, Bus JS, Holder JW (2008) Physiologically based pharmacokinetic modeling of chloroethane disposition in mice, rats, and women. Toxicol Sci 104:54–66
18. Gargas ML, Tyler TR, Sweeney LM, Corley RA, Weitz KK, Mast TJ, Paustenbach DJ, Hays SM (2000) A toxicokinetic study of inhaled ethylene glycol ethyl ether acetate and validation of a physiologically based pharmacokinetic model for rat and human. Toxicol Appl Pharmacol 165:63–73
19. Gargas ML, Tyler TR, Sweeney LM, Corley RA, Weitz KK, Mast TJ, Paustenbach DJ, Hays SM (2000) A toxicokinetic study of inhaled ethylene glycol monomethyl ether (2-ME) and validation of a physiologically based pharmacokinetic model for the pregnant rat and human. Toxicol Appl Pharmacol 165:53–62
20. Sweeney LM, Andersen ME, Gargas ML (2004) Ethyl acrylate risk assessment with a hybrid computational fluid dynamics and physiologically based nasal dosimetry model. Toxicol Sci 79:394–403
21. Edginton AN, Schmitt W, Voith B, Willmann S (2006) A mechanistic approach for the scaling of clearance in children. Clin Pharmacokinet 45:683–704
22. Johnson TN, Rostami-Hodjegan A, Tucker GT (2006) Prediction of the clearance of eleven drugs and associated variability in neonates, infants and children. Clin Pharmacokinet 45:931–956
23. Bjorkman S, Wada DR, Berling BM, Benoni G (2001) Prediction of the disposition of midazolam in surgical patients by a physiologically based pharmacokinetic model. J Pharm Sci 90:1226–1241
24. Harrison LI, Gibaldi M (1977) Physiologically based pharmacokinetic model for digoxin disposition in dogs and its preliminary application to humans. J Pharm Sci 66:1679–1683
25. Tod M, Lagneau F, Jullien V, Mimoz O (2008) A physiological model to evaluate drug kinetics in patients with hemorrhagic shock followed by fluid resuscitation. Application to amoxicillin-clavulanate. Pharm Res 25:1431–1439
26. Tsuji A, Nishide K, Minami H, Nakashima E, Terasaki T, Yamana T (1985) Physiologically based pharmacokinetic model for cefazolin in rabbits and its preliminary extrapolation to man. Drug Metab Dispos 13:729–739

27. Sugita O, Sawada Y, Sugiyama Y, Iga T, Hanano M (1982) Physiologically based pharmacokinetics of drug–drug interaction: a study of tolbutamide–sulfonamide interaction in rats. J Pharmacokinet Biopharm 10:297–316
28. Watanabe T, Kusuhara H, Maeda K, Shitara Y, Sugiyama Y (2009) Physiologically based pharmacokinetic modeling to predict transporter-mediated clearance and distribution of pravastatin in humans. J Pharmacol Exp Ther 328:652–662
29. Inoue S, Howgate EM, Rowland-Yeo K, Shimada T, Yamazaki H, Tucker GT, Rostami-Hodjegan A (2006) Prediction of in vivo drug clearance from in vitro data. II: potential inter-ethnic differences. Xenobiotica 36:499–513
30. Baillie TA, Cayen MN, Fouda H, Gerson RJ, Green JD, Grossman SJ, Klunk LJ, LeBlanc B, Perkins DG, Shipley LA (2002) Drug metabolites in safety testing. Toxicol Appl Pharmacol 182:188–196
31. Atrakchi AH (2009) Interpretation and considerations on the safety evaluation of human drug metabolites. Chem Res Toxicol 22:1217–1220
32. Shitara Y, Hirano M, Sato H, Sugiyama Y (2004) Gemfibrozil and its glucuronide inhibit the organic anion transporting polypeptide 2 (OATP2/OATP1B1:SLC21A6)-mediated hepatic uptake and CYP2C8-mediated metabolism of cerivastatin: analysis of the mechanism of the clinically relevant drug–drug interaction between cerivastatin and gemfibrozil. J Pharmacol Exp Ther 311:228–236
33. Isoherranen N, Hachad H, Yeung CK, Levy RH (2009) Qualitative analysis of the role of metabolites in inhibitory drug–drug interactions: literature evaluation based on the metabolism and transport drug interaction database. Chem Res Toxicol 22:294–298
34. Baillie TA (2009) Approaches to the assessment of stable and chemically reactive drug metabolites in early clinical trials. Chem Res Toxicol 22:263–266
35. Pang KS (2009) Safety testing of metabolites: expectations and outcomes. Chem Biol Interact 179:45–59
36. Pang KS, Morris ME, Sun H (2008) Formed and preformed metabolites: facts and comparisons. J Pharm Pharmacol 60:1247–1275
37. Pang KS, Gillette JR (1979) Sequential first-pass elimination of a metabolite derived from a precursor. J Pharmacokinet Biopharm 7:275–290
38. Pang KS (1985) A review of metabolite kinetics. J Pharmacokinet Biopharm 13:633–662
39. Pang KS, Kwan KC (1983) A commentary: methods and assumptions in the kinetic estimation of metabolite formation. Drug Metab Dispos 11:79–84
40. Sun H, Pang KS (2010) Physiological modeling to understand the impact of enzymes and transporters on drug and metabolite data and bioavailability estimates. Pharm Res 27:1237–1254
41. de Lannoy IA, Pang KS (1986) Presence of a diffusional barrier on metabolite kinetics: enalaprilat as a generated versus preformed metabolite. Drug Metab Dispos 14:513–520
42. de Lannoy IA, Pang KS (1987) Effect of diffusional barriers on drug and metabolite kinetics. Drug Metab Dispos 15:51–58
43. Pang KS, Cherry WF, Terrell JA, Ulm EH (1984) Disposition of enalapril and its diacid metabolite, enalaprilat, in a perfused rat liver preparation. Presence of a diffusional barrier for enalaprilat into hepatocytes. Drug Metab Dispos 12:309–313
44. Tirona RG, Pang KS (1996) Sequestered endoplasmic reticulum space for sequential metabolism of salicylamide. Coupling of hydroxylation and glucuronidation. Drug Metab Dispos 24:821–833
45. Tan E, Lu T, Pang KS (2001) Futile cycling of estrone sulfate and estrone in the recirculating perfused rat liver preparation. J Pharmacol Exp Ther 297:423–436
46. Schwab AJ, Tao L, Yoshimura T, Simard A, Barker F, Pang KS (2001) Hepatic uptake and metabolism of benzoate: a multiple indicator dilution, perfused rat liver study. Am J Physiol Gastrointest Liver Physiol 280:G1124–G1136
47. Chen J, Pang KS (1997) Effect of flow on first-pass metabolism of drugs: single pass studies on 4-methylumbelliferone conjugation in the serially perfused rat intestine and liver preparations. J Pharmacol Exp Ther 280:24–31
48. St-Pierre MV, Pang KS (1993) Kinetics of sequential metabolism. I. Formation and metabolism of oxazepam from nordiazepam and temazepam in the perfused murine liver. J Pharmacol Exp Ther 265:1429–1436
49. Sun H, Pang KS (2009) Disparity in intestine disposition between formed and preformed metabolites and implications: a theoretical study. Drug Metab Dispos 37:187–202
50. Xu X, Pang KS (1989) Hepatic modeling of metabolite kinetics in sequential and parallel pathways: salicylamide and gentisamide metabolism in perfused rat liver. J Pharmacokinet Biopharm 17:645–671

51. Cong D, Doherty M, Pang KS (2000) A new physiologically based, segregated-flow model to explain route-dependent intestinal metabolism. Drug Metab Dispos 28:224–235
52. Doherty MM, Pang KS (2000) Route-dependent metabolism of morphine in the vascularly perfused rat small intestine preparation. Pharm Res 17:291–298
53. Pang KS (2003) Modeling of intestinal drug absorption: roles of transporters and metabolic enzymes (for the Gillette Review Series). Drug Metab Dispos 31:1507–1519
54. Yang J, Jamei M, Yeo KR, Tucker GT, Rostami-Hodjegan A (2007) Prediction of intestinal first-pass drug metabolism. Curr Drug Metab 8:676–684
55. Tam D, Tirona RG, Pang KS (2003) Segmental intestinal transporters and metabolic enzymes on intestinal drug absorption. Drug Metab Dispos 31:373–383
56. Liu L, Pang KS (2006) An integrated approach to model hepatic drug clearance. Eur J Pharm Sci 29:215–230
57. Abu-Zahra TN, Pang KS (2000) Effect of zonal transport and metabolism on hepatic removal: enalapril hydrolysis in zonal, isolated rat hepatocytes in vitro and correlation with perfusion data. Drug Metab Dispos 28:807–813
58. Andersen ME, Birnbaum LS, Barton HA, Eklund CR (1997) Regional hepatic CYP1A1 and CYP1A2 induction with 2, 3, 7, 8-tetrachlorodibenzo-p-dioxin evaluated with a multicompartment geometric model of hepatic zonation. Toxicol Appl Pharmacol 144:145–155
59. Pang KS, Xu X, Morris ME, Yuen V (1987) Kinetic modeling of conjugations in liver. Fed Proc 46:2439–2441
60. Baillie TA, Halpin RA, Matuszewski BK, Geer LA, Chavez-Eng CM, Dean D, Braun M, Doss G, Jones A, Marks T, Melillo D, Vyas KP (2001) Mechanistic studies on the reversible metabolism of rofecoxib to 5-hydroxyrofecoxib in the rat: evidence for transient ring opening of a substituted 2-furanone derivative using stable isotope-labeling techniques. Drug Metab Dispos 29:1614–1628
61. Meffin PJ, Zilm DM, Veenendaal JR (1983) Reduced clofibric acid clearance in renal dysfunction is due to a futile cycle. J Pharmacol Exp Ther 227:732–738
62. Grubb NG, Rudy DW, Brater DC, Hall SD (1999) Stereoselective pharmacokinetics of ketoprofen and ketoprofen glucuronide in end-stage renal disease: evidence for a 'futile cycle' of elimination. Br J Clin Pharmacol 48:494–500
63. Hansel SB, Morris ME (1996) Hepatic conjugation/deconjugation cycling pathways. Computer simulations examining the effect of Michaelis–Menten parameters, enzyme distribution patterns, and a diffusional barrier on metabolite disposition. J Pharmacokinet Biopharm 24:219–243
64. Kauffman FC, Whittaker M, Anundi I, Thurman RG (1991) Futile cycling of a sulfate conjugate by isolated hepatocytes. Mol Pharmacol 39:414–420
65. Ratna S, Chiba M, Bandyopadhyay L, Pang KS (1993) Futile cycling between 4-methylumbelliferone and its conjugates in perfused rat liver. Hepatology 17:838–853
66. Xu X, Selick P, Pang KS (1993) Nonlinear protein binding and enzyme heterogeneity: effects on hepatic drug removal. J Pharmacokinet Biopharm 21:43–74
67. Sun H, Zeng YY, Pang KS (2010) Interplay of phase II enzymes and transporters in futile cycling: influence of multidrug resistance-associated protein 2-mediated excretion of estradiol 17β-D-glucuronide and its 3-sulfate metabolite on net sulfation in perfused TR- and Wistar rat liver preparations. Drug Metab Dispos 38:769–780
68. Chen S, Fan J, Pang KS (2010) Physiologically-based pharmacokinetic (PBPK) models for the description of sequential metabolism of codeine to morphine and morphine 3-glucuronide in man and rat, AAPS Annual Meeting, New Orleans, LA, 2010; Abstract #R6395
69. Chiu WA, Okino MS, Evans MV (2009) Characterizing uncertainty and population variability in the toxicokinetics of trichloroethylene and metabolites in mice, rats, and humans using an updated database, physiologically based pharmacokinetic (PBPK) model, and Bayesian approach. Toxicol Appl Pharmacol 241:36–60
70. Gerlowski LE, Jain RK (1983) Physiologically based pharmacokinetic modeling: principles and applications. J Pharm Sci 72:1103–1127
71. Verwei M, van Burgsteden JA, Krul CA, van de Sandt JJ, Freidig AP (2006) Prediction of in vivo embryotoxic effect levels with a combination of in vitro studies and PBPK modelling. Toxicol Lett 165:79–87
72. Barton HA, Clewell HJ 3rd (2000) Evaluating noncancer effects of trichloroethylene: dosimetry, mode of action, and risk assessment. Environ Health Perspect 108(Suppl 2):323–334
73. Sweeney LM, Kirman CR, Gargas ML, Dugard PH (2009) Contribution of trichloroacetic acid to liver tumors observed in perchloroethylene (perc)-exposed mice. Toxicology 260:77–83

74. Yang RS, el-Masri HA, Thomas RS, Constan AA, Tessari JD (1995) The application of physiologically based pharmacokinetic/pharmacodynamic (PBPK/PD) modeling for exploring risk assessment approaches of chemical mixtures. Toxicol Lett 79:193–200
75. Andersen ME, Clewell HJ 3rd, Gargas ML, Smith FA, Reitz RH (1987) Physiologically based pharmacokinetics and the risk assessment process for methylene chloride. Toxicol Appl Pharmacol 87:185–205
76. Clewell HJ, Gentry PR, Gearhart JM, Allen BC, Andersen ME (2001) Comparison of cancer risk estimates for vinyl chloride using animal and human data with a PBPK model. Sci Total Environ 274:37–66
77. Reitz RH, Gargas ML, Andersen ME, Provan WM, Green TL (1996) Predicting cancer risk from vinyl chloride exposure with a physiologically based pharmacokinetic model. Toxicol Appl Pharmacol 137:253–267
78. Clewell HJ 3rd, Andersen ME, Wills RJ, Latriano L (1997) A physiologically based pharmacokinetic model for retinoic acid and its metabolites. J Am Acad Dermatol 36:S77–S85
79. Frederick CB, Bush ML, Lomax LG, Black KA, Finch L, Kimbell JS, Morgan KT, Subramaniam RP, Morris JB, Ultman JS (1998) Application of a hybrid computational fluid dynamics and physiologically based inhalation model for interspecies dosimetry extrapolation of acidic vapors in the upper airways. Toxicol Appl Pharmacol 152:211–231
80. Frederick CB, Lomax LG, Black KA, Finch L, Scribner HE, Kimbell JS, Morgan KT, Subramaniam RP, Morris JB (2002) Use of a hybrid computational fluid dynamics and physiologically based inhalation model for interspecies dosimetry comparisons of ester vapors. Toxicol Appl Pharmacol 183:23–40
81. Andersen ME, Sarangapani R, Frederick CB, Kimbell JS (1999) Dosimetric adjustment factors for methyl methacrylate derived from a steady-state analysis of a physiologically based clearance-extraction model. Inhal Toxicol 11:899–926
82. Sarangapani R, Teeguarden JG, Cruzan G, Clewell HJ, Andersen ME (2002) Physiologically based pharmacokinetic modeling of styrene and styrene oxide respiratory-tract dosimetry in rodents and humans. Inhal Toxicol 14:789–834
83. Evans MV, Chiu WA, Okino MS, Caldwell JC (2009) Development of an updated PBPK model for trichloroethylene and metabolites in mice, and its application to discern the role of oxidative metabolism in TCE-induced hepatomegaly. Toxicol Appl Pharmacol 236:329–340
84. Sarangapani R, Teeguarden J, Andersen ME, Reitz RH, Plotzke KP (2003) Route-specific differences in distribution characteristics of octamethylcyclotetrasiloxane in rats: analysis using PBPK models. Toxicol Sci 71:41–52
85. Corley RA, Bartels MJ, Carney EW, Weitz KK, Soelberg JJ, Gies RA, Thrall KD (2005) Development of a physiologically based pharmacokinetic model for ethylene glycol and its metabolite, glycolic acid, in rats and humans. Toxicol Sci 85:476–490
86. McMullin TS, Hanneman WH, Cranmer BK, Tessari JD, Andersen ME (2007) Oral absorption and oxidative metabolism of atrazine in rats evaluated by physiological modeling approaches. Toxicology 240:1–14
87. Clewell RA, Kremer JJ, Williams CC, Campbell JL Jr, Andersen ME, Borghoff SJ (2008) Tissue exposures to free and glucuronidated monobutylyphthalate in the pregnant and fetal rat following exposure to di-*n*-butylphthalate: evaluation with a PBPK model. Toxicol Sci 103:241–259
88. Sweeney LM, Thrall KD, Poet TS, Corley RA, Weber TJ, Locey BJ, Clarkson J, Sager S, Gargas ML (2008) Physiologically based pharmacokinetic modeling of 1,4-dioxane in rats, mice, and humans. Toxicol Sci 101:32–50
89. Zhang X, Quinney SK, Gorski JC, Jones DR, Hall SD (2009) Semiphysiologically based pharmacokinetic models for the inhibition of midazolam clearance by diltiazem and its major metabolite. Drug Metab Dispos 37:1587–1597
90. Rietjens IM, Punt A, Schilter B, Scholz G, Delatour T, van Bladeren PJ (2010) In silico methods for physiologically based biokinetic models describing bioactivation and detoxification of coumarin and estragole: implications for risk assessment. Mol Nutr Food Res 54:195–207